Effect of Extrinsic Electric Fields upon Dielectronic Recombination: Mg^{1+}

K. LaGattuta and Y. Hahn
Physics Department, University of Connecticut, Storrs, Connecticut 06268
(Received 9 May 1983)

Recently, large discrepancies have appeared between theoretical predictions and experimental measurements of dielectronic recombination cross sections (σ^{DR}) for Mg^{1+} targets. This disagreement has provoked new work aimed at understanding, more fully, the effect of applied fields upon the process. This Letter reports calculations of σ^{DR} for Mg^{1+} in a small applied electric field. The field effect is large enough to bring the experimental σ^{DR} into much closer agreement with the theory.

PACS numbers: 32.80.Hd, 52.20.Fs

In this Letter we describe the results of an approximate calculation of the dielectronic recombination (DR) rate coefficient (α^{DR}) and cross section (σ^{DR}) for Mg^{1+} targets, when the targets are immersed in an externally applied static homogeneous electric field (F). The method employed is similar to one described by Huber and Bottcher.[1] Related work by Jacobs, Davis, and Kepple[2] and by Burgess and Summers[3] appeared earlier. We find that σ^{DR} values for Mg^{1+}, calculated with F in the range 5–50 V/cm, are enhanced by as much as a factor of ~10 over the values calculated with zero field.

Recently reported crossed-beam measurements[4] of σ^{DR} for Mg^{1+} are a factor of ~7 higher than the theoretical prediction.[5] This prediction was, however, only appropriate for the case $F=0$. In the experiment of the JILA group,[4] a 0.02-T magnetic field was applied parallel to the electron beam axis to inhibit beam spread. Depending upon the angle between the electron and the ion beams, this translates into an electric field of $\lesssim 24$ V/cm, in the ion-beam rest frame. Consequently, cross sections calculated for $F=0$ may not be relevant to this experiment.

For the Mg^{1+} system in an applied electric field, the processes we considered were

$$3s + e_c \rightarrow (3p)(nkm) \rightarrow (3s)(nkm) + \text{photon}, \tag{1}$$

where e_c is the energy of the continuum electron. During collision the $3s$ target electron is excited to $3p$ (neglecting exchange) and the continuum particle is captured into a high Rydberg state (HRS),[6] labeled by principal, electric field, and magnetic quantum numbers n, k, and m, respectively. Parabolic coordinates[7] were used to describe the HRS electron:

$$|nkm\rangle = \sum_{l=0}^{n-1} (-)^{1-n-m}(2l+1)^{1/2} \begin{pmatrix} \frac{1}{2}(n-1) & \frac{1}{2}(n-1) & l \\ \frac{1}{2}(m-k) & \frac{1}{2}(m+k) & -m \end{pmatrix} |nlm\rangle. \tag{2}$$

The rate coefficient was given by

$$\alpha^{DR} = \sum_{n=3}^{\infty} \alpha_n{}^{DR}, \tag{3}$$

where

$$\alpha_n{}^{DR} = 3\left(\frac{4\pi}{k_B T}\right)^{3/2} a_0{}^3 A_r(3p \rightarrow 3s) \exp\left(-\frac{e_c}{k_B T}\right) \sum_{k,m} \frac{A_a(n,k,m)}{A_a(n,k,m) + A_r(3p \rightarrow 3s)}. \tag{4}$$

In (4) we assume that m is a good quantum number even though the core $3p$ electron possesses orbital angular momentum. Because of this approximation, the $F \rightarrow 0$ light of (4) is ~50% higher than the LS-coupled zero-field result.[5] There is no explicit spin dependence since the vast majority of captures are to $n \gg 1$ and $l \gtrsim 1$, where spin effects should be small. The Auger probability, A_a, was computed from

$$A_a(n,k,m) = \frac{2\pi}{9\tau_0} \sum_{l=0}^{n-1} \begin{pmatrix} \frac{1}{2}(n-1) & \frac{1}{2}(n-1) & l \\ \frac{1}{2}(m-k) & \frac{1}{2}(m+k) & -m \end{pmatrix}^2 [(l+1)R_1{}^2(l_c = l+1) + lR_1{}^2(l_c = l-1)], \tag{5}$$

where $\tau_0 = 2.42 \times 10^{-17}$ sec,

$$R_1{}^2(l_c) = |\langle (3s)_i (e_c l_c)_j | (1/r_{ij}) | (3p)_i (nl)_j \rangle|^2$$

in atomic units, and for simplicity we assumed no preferred direction for the incoming electron. Equation (5) is an exact result for the states (2) when exchange is neglected and after averaging over the orientation of the continuum electron wave vector. A more accurate procedure should preserve this orientation with respect to the electric field. In this case, cross terms may appear in (5). The radiative probability A_r was

$$A_r(3p \to 3s) = (\alpha_0^3/6\tau_0)(\Delta E_{3p,3s})^3(r_{3p,3s})^2/3 \simeq 2.80\times10^8 \text{ sec}^{-1}. \tag{7}$$

Throughout, all energies are in rydbergs.
The cross section averaged over an energy bin size of Δe_c is[5]

$$\bar{\sigma}_n^{\,DR} = 4.06\times10^{-9}(k_B T)^{3/2} \exp(e_c/k_B T\,\alpha_n^{\,DR})/(e_c\,\Delta e_c) \text{ cm}^2, \tag{8}$$

where

$$\bar{\sigma}_n^{\,DR} \equiv (1/\Delta e_c)\int_{e_c-\frac{1}{2}\Delta e_c}^{e_c+\frac{1}{2}\Delta e_c} de_c'\,\sigma_n^{\,DR}(e_c'). \tag{9}$$

So far, the size of the electric field has not entered explicitly. The field-strength dependence should be of two types. First, for fixed n the probability of field ionization, A_F, will vary as[8]

$$A_F = \left(\frac{4}{\tau_0 a_0 F n^2}\right)\exp(-2/3a_0 F n^3), \tag{10}$$

where F is in volts per centimeter. This is the maximum A_F value, obtained for $k = 1-n$ and $m = 0$; explicit k and m dependence was not considered. Equation (10) is valid provided that $10a_0 F n^3 \lesssim 1$. Second, F dependence of the l-mixing coefficients in the parabolic basis should be included [see Eq. (2)].

Hence, two modifications of Eq. (4) are required. We need to include the probability of field ionization in the denominator according to

$$\alpha_n^{\,DR} = 3\left(\frac{4\pi}{k_B T}\right)^{3/2} a_0^3 A_r \exp\left(-\frac{e_c}{k_B T}\right)\sum_{k,m}\frac{A_a(n,k,m)}{A_a(n,k,m)+A_r+A_F}\,\frac{\text{cm}^3}{\text{sec}}, \tag{11}$$

and we need to account systematically for the fact that the parabolic basis states may be diluted, for given n and F, by spherical basis states of low l.

To deal with this last point we compared the separation in energy of the various l levels, for fixed n in a spherical basis at $F = 0$, with the field-induced energy shifts of these levels. Slater integrals were used to describe, approximately, the relative energies of the l levels at $F = 0$:

$$\delta E_{nl} \equiv \langle (3p)_i (nl)_j; L | (1/r_{ij}) | (3p)_i (nl)_j \rangle \text{ (a.u.)}$$
$$= 3(2l+1)\sum_\nu (-)^{L+\nu} R_\nu \begin{pmatrix} 1 & 1 & \nu \\ 0 & 0 & 0 \end{pmatrix}\begin{pmatrix} l & l & \nu \\ 0 & 0 & 0 \end{pmatrix}\begin{Bmatrix} 1 & l & L \\ l & 1 & \nu \end{Bmatrix}. \tag{12}$$

In (12), $(3p)(nl)$ are coupled into a state of total L and Coulomb wave functions were used to evaluate the radial integrals, R_0 and R_2. Checks of this formula against Hartree-Fock energies for $n = 10$, $L = l$, and $l = 1, 2, 3$ showed it to be reliable for these cases. We assumed that it would be reliable for all $l \gtrsim 1$ and $n \gtrsim 10$, if $L = l$.

As a measure of the field-induced energy shifts of the levels labeled by n and l, we used the formula[9]

$$\Delta E_{nl} = F r_{nl,nl}$$
$$= (a_0/2)F[3n^2 - l(l+1)] \text{ eV}, \tag{13}$$

where F is in volts per centimeter. If, at a given F, n, and $l = l_m$, we found that $\Delta E_{nl_m} \geq \delta E_{nl_m} - \delta E_{n\,n-1}$, then we assumed that all states with $l \geq l_m$ were completely mixed and that the mixing coefficients were given by Eq. (2). In practice, for the cases of interest, $l_m \ll n$ so that $\Delta E_{nl_m} \simeq \Delta E_{n0}$ and the condition for mixing became $\Delta E_{n0} \geq \delta E_{nl_m}$; see Table I. States with $l < l_m$ were deleted from the sum over l in Eq. (5), and their contribution to the overall $\alpha_n^{\,DR}$ values estimated separately with use of spherical basis functions. In the application of the approximate criterion described here, it seems immaterial that M_L rather than L might be the good quantum number in field. The criterion is not intended to be precise.

In Fig. 1 we plot values of $\alpha_n^{\,DR}$ versus n for parabolic basis functions; the effect of limiting

TABLE I. List of l values mixed by electric field of 24 V/cm, as a function of n; Mg^{1+} $(3p)(nl)$ configuration; l values mixed are for $l \geq l_m$; results based upon predictions of Eqs. (12) and (13); HF denotes Hartree-Fock energy.

n	$10^4\Delta E_{n0}$ (eV)	$10^4\delta E_{nl}$; $L=l$ (eV)	l_m
60	6.9		0
55	5.8	4.0 ($l=0$) [HF]	0
50	4.8	5.3 ($l=0$) [HF]	
		4.0 ($l=1$)	1
45	3.9	5.5 ($l=1$)	
		1.1 ($l=2$)	2
40	3.1	1.6 ($l=2$)	2
35	2.3	2.3 ($l=2$)	
		0.8 ($l=3$)	3
30	1.7	1.3 ($l=3$)	3
25	1.2	2.3 ($l=3$)	
		1.1 ($l=4$)	4
20	0.8	1.1 ($l=5$)	
		0.7 ($l=6$)	6
15	0.4	0.5 ($l=9$)	$\gtrsim 9$

the range of l values mixed is displayed. For reference we include a plot of α_n^{DR} computed with spherical basis functions in zero field. Figure 2 displays the final results of our calculation based upon Eq. (11). All of the derived field dependence is included; i.e., both as pertains to n- and F-dependent l mixing (Table I) and as pertains to field ionization. Results for $F \lesssim 1$ V/cm are dubious but the correct limit for α_n^{DR} is obtained as $F \to 0$. [However, see the remarks just after Eq. (4).] Following directly from Fig. 2, and based upon Eqs. (8) and (9), we plot in Fig. 3 the DR cross section, σ_n^{DR} vs e_c, for $F = 24$ V/cm. Variations of F between 6 V/cm and 48 V/cm make only small (~ 20%) changes in cross section. The cross section has been convolved with a Lorentzian profile of 0.30 eV full width at half maximum and a cutoff has been imposed at $n = 64$. This simulates the experimental conditions set by the JILA group. Experimental data

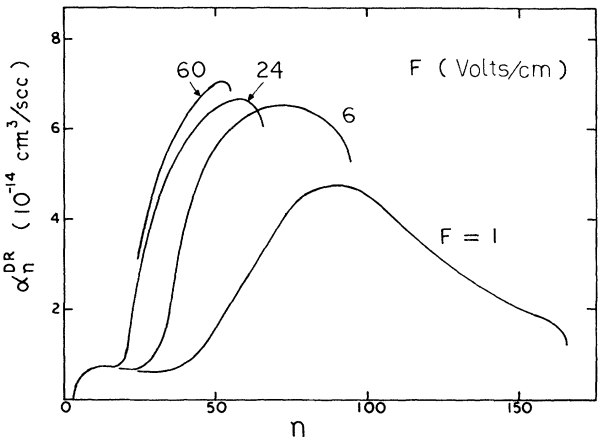

FIG. 2. α_n^{DR} vs n for g.s. Mg^{1+} target ($\Delta n = 0$) excitation; effect of electric field, F, included explicitly, with l mixing and field ionization accounted for via Eqs. (10)–(13); all are at $k_BT = 7$ Ry.

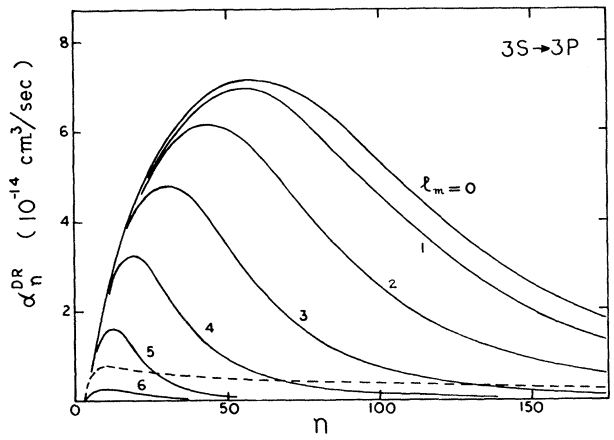

FIG. 1. α_n^{DR} vs n for ground state (g.s.) Mg^{1+} target ($\Delta n = 0$) excitation. Solid curves: parabolic basis functions, no field ionization, for various l_m values (l values are mixed for $l \geq l_m$); dashed curve: spherical basis functions, LS coupling, zero field; all are at $k_BT = 7$ Ry.

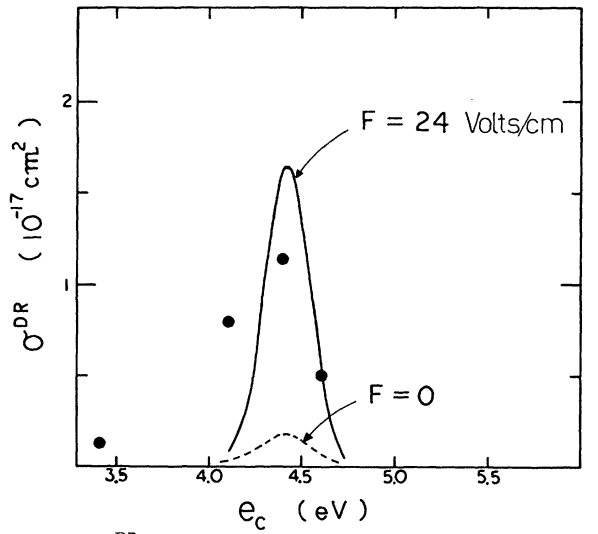

FIG. 3. σ^{DR} vs e_c for g.s. Mg^{1+} target ($\Delta n = 0$) excitation; l mixing and field ionization are accounted for via Eqs. (10)–(13); cutoff applied at $n = 64$; the result is convolved with a Lorentzian of 0.30 eV full width at half maximum.

points from this group are included in the figure.

Agreement between theory and experiment is now much improved, but clearly further work is still necessary. The next step may involve a more careful mixing of spherical and parabolic basis functions to account for l-level nondegeneracy; i.e., an explicit diagonalization. Also, as mentioned, the dependence of σ^{DR} upon the angle between the electric field vector and the electron initial momentum vector should be included. The problem of field-induced mixing among the n levels occurs as n approaches the field-ionization limit (see Table I). We judge, however, that this is not an important effect since the number of states accessible to capture is not increased by the mixing. Overlapping resonances do occur for the lowest l values ($l=0, 1$) at each n, but this seems to lead to only a small ($\sim 10\%$) increase in cross section.

Behavior similar to that displayed in Figs. 1 and 2 was predicted in Ref. 1 for DR of He^{1+}. However, in that paper emphasis was placed upon the influence of the diamagnetic potential for magnetic fields of the order of several teslas. By deduction from that work, the diamagnetic potential should have a negligible influence upon σ^{DR} for Mg^{1+}, if $B=0.02$ T. Considering the large enhancement in σ^{DR} depicted in Fig. 3, we do not confirm the area-conserving hypothesis of Ref. 1. Also, our preliminary calculations of α^{DR} for Fe^{23+} confirm the prediction of Ref. 2 for the effect of an applied field upon DR. However, our derived $\alpha_n{}^{DR}$ versus n is at variance with that work.

We expect that considerations similar to those described in this paper will reduce the rather large discrepancies found between theory and experiment for DR in C^{1+} systems.[10,11] If so, then the experiments in which DR cross sections are being measured give an incentive to reexamine calculations of α^{DR}, since DR rates will be used for the modeling of plasmas in an environment of strong electric and magnetic fields.

This work was supported in part by a grant from the U. S. Department of Energy.

[1]W. A. Huber and C. Bottcher, J. Phys. B 13, L399 (1980).

[2]V. L. Jacobs, J. Davis, and P. C. Kepple, Phys. Rev. Lett. 37, 1390 (1976).

[3]A. Burgess and H. P. Summers, Astrophys. J. 157, 1007 (1969).

[4]D. S. Belić, G. H. Dunn, T. J. Morgan, D. W. Mueller, and C. Timmer, Phys. Rev. Lett. 50, 339 (1983).

[5]K. LaGattuta and Y. Hahn, J. Phys. B 15, 2101 (1982).

[6]K. LaGattuta and Y. Hahn, Phys. Lett. 84A, 468 (1981).

[7]B. W. Shore and D. H. Menzel, *Principles of Atomic Spectra* (Wiley, New York, 1968), pp. 498–503.

[8]L. D. Landau and E. M. Lifshitz, *Quantum Mechanics* (Pergamon, New York, 1958), pp. 257, 258.

[9]H. A. Bethe and E. E. Salpeter, *Quantum Mechanics of One and Two Electron Atoms* (Springer-Verlag, Berlin, 1957), p. 17.

[10]K. LaGattuta and Y. Hahn, Phys. Rev. Lett. 50, 668 (1983).

[11]J. B. A. Mitchell, C. T. Ng, J. L. Forand, D. P. Levac, R. E. Mitchell, A. Sen, D. B. Miko, and J. Wm. McGowan, Phys. Rev. Lett. 50, 335 (1983).